

## Specific Binding Sites for a Parvovirus, Minute Virus of Mice, on Cultured Mouse Cells

P. LINSEY,\* HELEN BRUNING, AND R. W. ARMENTROUT

*Department of Biological Chemistry, University of Cincinnati Medical Center, Cincinnati, Ohio 45267*

Received for publication 30 March 1977

The early interactions between parvoviruses and host cells have not been extensively described previously. In this study we have characterized some aspects of viral binding to the cell surface and demonstrated the existence of specific cellular receptor sites for minute virus of mice (MVM) on two murine cell lines that are permissive for viral growth. The interaction had a pH optimum of 7.0 to 7.2, and both the rate and extent of the reactions were slightly affected by temperature. Mouse A-9 cells (L-cell derivative) had  $\sim 5 \times 10^5$  specific MVM binding sites per cell, and Friend erythroleukemia cells had  $1.5 \times 10^5$  MVM sites per cell. In contrast, the nonpermissive mouse lymphoid cell line L1210 lacked specific viral receptors. Also, cloned lines of A-9 cells resistant to viral infection have been isolated. One of these lines lacked the "specific" virus attachment sites but exhibited low levels of nonsaturable virus binding. Based on these examples, infectivity is correlated with the presence of specific viral receptors on the cell surface.

We have looked at the initial interaction between minute virus of mice (MVM) and several murine tissue culture cell lines in order to characterize and quantify a specific virus-binding site. MVM is a parvovirus, a class of small viruses that contain a linear single-stranded DNA genome. Very little information concerning early parvovirus host cell interactions has been previously reported (19). However, the binding of picornaviruses to cells has been extensively studied and is in some respects analogous to the parvovirus system. Parvoviruses and picornaviruses are roughly the same size ( $\sim 17$  to  $30$  nm in diameter), and they both consist of an icosahedral protein capsid surrounding a single-stranded nucleic acid genome (RNA in the case of picornaviruses). The initial interaction of picornaviruses such as poliovirus with susceptible host cells has been characterized. The number of specific binding sites per cell is known ( $\sim 10^4$ /cell) (10, 14, 15), and the presence of specific cellular binding sites in part explains the cytological specificity of poliovirus infections. There is evidence that parvoviruses may be tissue specific as well (3, 12), and this report is the first evidence for a relationship between infectivity and the presence of specific virus-binding sites on the host cell.

### MATERIALS AND METHODS

**Virus stocks.** All cell lines were free of mycoplasma as determined periodically by autoradiography. Plaque-purified MVM was the generous gift of

Peter Tattersall. MVM labeled in its DNA with [*methyl*- $^3$ H]thymidine was grown in RT-7 cells (previously described [18]). Randomly growing infected cells were labeled for 48 h during the interval of maximum viral encapsulation. Half-confluent monolayers of RT-7 cells in Corning T-flasks were infected with MVM purified from the 110S region of a sucrose gradient. The virus was adsorbed to cells in phosphate-buffered saline (PBS) at  $37^\circ\text{C}$  for 2 h. The monolayers were then fed with fresh F-11 (minimal essential medium, Grand Island Biological Co. [GIBCO]) with 5% heat-inactivated fetal calf serum and 100 U of penicillin and 100  $\mu\text{g}$  of streptomycin per ml. Twenty-four hours after infection the monolayers were subcultured and refed with fresh medium containing 25  $\mu\text{Ci}$  of [*methyl*- $^3$ H]thymidine per ml. Forty-eight hours later the monolayers were harvested into 0.01 M Tris buffer (pH 9.0), disrupted by sonic treatment, and extracted twice with 5 volumes of Freon. The aqueous phase was brought to a final concentration of 10 mM  $\text{MgCl}_2$ . DNase (Worthington Biochemicals Corp.) was added to 0.1 mg/ml, and the mixture was incubated in a  $37^\circ\text{C}$  water bath for 60 min. The crude preparation was then dialyzed at  $4^\circ\text{C}$  overnight against  $3 \times 1$ -liter changes of 0.01 M Tris-0.005 M EDTA (pH 9.0) buffer. The preparation was then layered onto 37-ml continuous 15 to 30% sucrose gradients and centrifuged in an SW-27 rotor at 25,000 rpm and  $4^\circ\text{C}$  for 6.5 h. The 110S peak of full virus was located by a combination of the optical density at 260 nm, the hemagglutinin activity, and the DNase-resistant, acid-insoluble radioactivity assayed across the gradient as previously described (18). The concentration of virus particles in the virus preparations was measured by the optical density at 280 nm and calculated from an  $E_{280}^{1\%}$  of 71.2 as described by Tattersall et al. (21). Essentially the

same results were obtained when the concentration of particles was estimated from the protein concentration as determined by fluorescence (5) and using a value of  $4 \times 10^6$  daltons of protein per mol of particles. Infectivity of preparations of this type is typically 1 infectious unit per  $4 \times 10^2$  to  $6 \times 10^2$  particles, as measured by 50% tissue culture infective dose or plaque assay.

A-9 cells, a suspension culture derivative of mouse L-cells (13), were grown in F-11 (minimal essential medium, GIBCO) supplemented with 10% heat-inactivated fetal calf serum and 100 U of penicillin and 100  $\mu$ g of streptomycin per ml in suspension at densities from  $5 \times 10^4$  to  $5 \times 10^5$ /ml. These cells are permissive for viral growth (20) and represent the model system used to define several parameters of virus-cell binding in this study.

Murine Friend-745 erythroleukemia cells (Friend virus-transformed spleen cells) (6, 8) were provided by K. Lowenhaupt. These cells are permissive for viral growth (16a) and can be induced to undergo erythropoietic "differentiation" in culture by dimethyl sulfoxide ( $\text{Me}_2\text{SO}$ ) treatment (6). These cells are suspension adapted and were grown in Ham F-12 (GIBCO) supplemented with 10% fetal calf serum at suspension densities of  $2 \times 10^4$  to  $4 \times 10^5$ /ml. These cells were induced by the addition of 1.8%  $\text{Me}_2\text{SO}$  to  $4 \times 10^4$  cells per ml in fresh F-12. The course of induction was monitored by scoring the percentage of cells that were positive for hemoglobin by the benzidine staining technique (6).

The mouse lymphoid cell line L1210 was the gift of J. McCormick. These cells do not support MVM growth (16a) and constitute the negative control for virus binding used in this study. L1210 cells are also grown in suspension in RPMI 1640 (GIBCO) supplemented with 10% heat-inactivated fetal calf serum at densities of  $2 \times 10^4$  to  $5 \times 10^5$ /ml.

**Binding assay.** Binding of radiolabeled virus to cells was performed in suspension with periodic gentle mixing to keep cells suspended. Reactions were carried out in sterile Corning disposable polystyrene conical centrifuge tubes, as described for each experiment in Results. Unless otherwise specified, for each data point a known quantity of virus in a small volume (i.e., 5 to 50  $\mu$ l) was added to  $2 \times 10^5$  cells in 1 ml of buffer. The virus was stored at  $-20^\circ\text{C}$  in the sucrose solution of the isolation gradient, conditions which prevented viral aggregation. After the appropriate incubation time, the sample was filtered through a 25-mm Nuclepore filter with 5.0- $\mu$ m pore size, and the filter, which retained the cells, was washed twice with 20 ml of ice-cold buffer. The filter was then air-dried, solubilized with Soluene-100 (Packard), and counted by scintillation spectrophotometry in toluene-based scintillation cocktail. Specific activity of virus preparations was determined by precipitation of a sample of virus in 10% trichloroacetic acid on a Whatman GFA glass filter, digested with Soluene, and counted by scintillation. When radiolabeled virus particles were directly filtered, less than 0.1% of the input radioactivity was retained by the filter. The DNase lability of trichloroacetic acid-precipitable counts in the frozen virus preparations was negligible.

**Selection of resistant cells.** A-9 cells resistant to MVM infection were selected by allowing surviving cells from an infection to grow out and cloning cells from the resultant cell population. A-9 cells were grown in monolayer in F-11 (minimal essential medium, GIBCO) supplemented with 5% heat-inactivated fetal calf serum and 100 U of penicillin and 100  $\mu$ g of streptomycin per ml. The monolayers were infected as described for RT-7 cell infection (18). After lysis of most cells due to infection, a few survivors were noted and allowed to repopulate the original culture vessel over a period of 3 to 4 weeks. After regrowth of the monolayer, the culture now enriched for cells resistant to MVM infection was trypsinized with 0.25% trypsin in PBS (GIBCO) and diluted to 1 cell per 10  $\mu$ l and seeded into microwell cloning plates at 10  $\mu$ l/well. During outgrowth of the clones, each culture was monitored for the production of viral proteins by hemagglutination assay, and only those cultures free of viral protein were subsequently tested for susceptibility to infection using a 50% tissue culture infective dose assay. Clones were also screened for virus binding using the assay systems described in Results.

**Electron microscopy.** Normal A-9 cell monolayers in 60-mm culture dishes were rinsed in PBS at  $4^\circ\text{C}$ , and  $10^6$  110S MVM particles per cell were added in a total volume of 1 ml of PBS and allowed to adsorb at  $4^\circ\text{C}$  for 2 h. The monolayers were then washed in ice-cold PBS several times, fixed in 3% glutaraldehyde in phosphate buffer for 1 h at  $4^\circ\text{C}$ , and postfixed in 1% osmic acid. The monolayers were embedded in Luft Epon mixture and sectioned with a DuPont diamond knife perpendicular to the plane of growth, as described by Anderson et al. (1). Electron micrographs were taken on a JEOL JEM 100B at 60-kV acceleration voltage.

## RESULTS

Several conditions of the virus-binding reaction were examined to optimize the conditions of the assay. It was important to minimize uptake of virus into cells. As uptake of particles by cells can be reduced by working at low temperatures, the effect of temperature on the virus-binding interactions was examined. In Fig. 1,  $10^5$  virus particles per cell were added to  $2.2 \times 10^5$  A-9 cells in 1 ml of PBS at either  $4$  or  $21^\circ\text{C}$ , and the mixture was allowed to incubate for 30 s or 1, 3, 5, 15, 30, 60, or 120 min. At the end of the incubation time, the sample was filtered as described in Materials and Methods and washed with ice-cold PBS, and the cell-bound counts per minute were measured. At both  $4$  and  $21^\circ\text{C}$  the reaction appears to consist of a rapid component within the first 30 min and a slow component that continues for at least 2 h. Adsorption times of up to 4 h have been examined at  $4^\circ\text{C}$ , and the slow reaction appears to continue indefinitely (not shown). As temperature appears to have only a slight effect on the

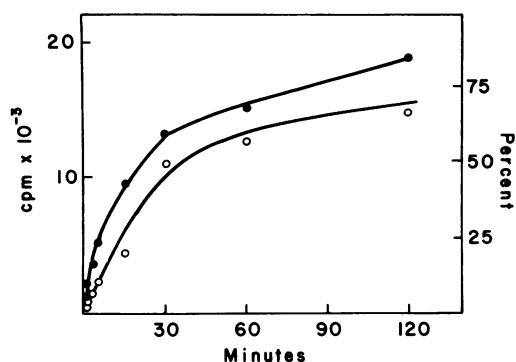


FIG. 1. Effect of temperature on the binding of MVM to A-9 cells in suspension. A total of  $2 \times 10^5$  cells in PBS, pH 7.2, were reacted with  $10^4$  [ $^3\text{H}$ ]thymidine-labeled 110S MVM per cell for 30 s to 2 h at either 21 or 4°C. The reaction was stopped by filtration of the cell suspension through 25-mm Nucleopore filters with a 5.0- $\mu\text{m}$  pore size. Cell-associated tritium counts per minute are plotted versus the time. Temperature affects the rate of the reaction and the shape of the curve only slightly. Symbols: (○) 4°C; (●) 21°C.

extent of virus binding, subsequent binding experiments were performed at 4°C for 2 h as the standard conditions.

Little if any of the virus bound to cells at 4°C appears to be taken up during the 2-h incubation period, as 78% of the cell-associated counts can be removed by a brief wash (5 min) in  $\text{Ca}^{2+}$ ,  $\text{Mg}^{2+}$ -free PBS with 0.001 M EDTA (Table 1). Treatment of this sort has no observable effects on plating efficiency of the cells. Thus, the binding assay appears to measure primarily surface attachment and is not significantly complicated by uptake into cells. This conclusion is supported by the fact that virus previously bound to the cell surface can be competitively displaced by subsequently added unlabeled virus (Fig. 2). In this experiment a subsaturating amount of labeled virus ( $10^4$  particles per cell) was allowed to bind to cells at 4°C for 2 h. Increasing concentrations of unlabeled virus were then added to the cell suspension. After 1 h, the amount of residual label bound to the cells was measured. It can be seen from Fig. 2, curve B, that the amount of cell-bound label remains constant until the input multiplicity exceeds  $5 \times 10^5$  particles per cell. However, once this saturation level has been exceeded, the additional unlabeled virus effectively competes with the labeled virus for attachment to the cell surface. These results indicate that binding of virus to the cell surface is most likely a reversible reaction and that a major portion of the virus is probably bound at the cell surface under the conditions of the binding assay.

A critical question in measuring any binding

TABLE 1. Effect of wash treatment on amount of virus bound to cells<sup>a</sup>

Treatment	cpm bound		Avg	% of total
	Sample 1	Sample 2		
Control	1,248	1,186	1,217	100
EDTA wash	219	334	276	22

<sup>a</sup> Four samples each containing  $2 \times 10^5$  cells suspended in 1 ml of PBS at 4°C were reacted with  $10^5$  [ $^3\text{H}$ ]thymidine-labeled MVM particles per cell for 2 h. At the end of the incubation time the samples were filtered and washed as described in the text. Two samples were then washed for 5 minutes (slow filtration) in  $\text{Ca}^{2+}$ ,  $\text{Mg}^{2+}$ -free PBS with 1 mM EDTA. A total of 78% of the cell-associated counts was washed off by this treatment.

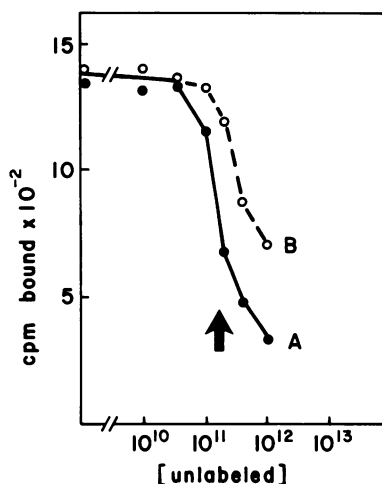


FIG. 2. Curve of competition between binding labeled and unlabeled MVM; A-9 cells suspended in PBS at 4°C were reacted with a fixed quantity of [ $^3\text{H}$ ]thymidine-labeled MVM ( $2.4 \times 10^9$  particles). In the first case (curve A, ●) the labeled virus was mixed with increasing amounts of unlabeled virus prior to adsorption to cells ( $2 \times 10^5$ ). In the second instance (curve B, ○) the labeled virus was allowed to adsorb to the cells ( $1.7 \times 10^5$ ) for 2 h, and increasing amounts of unlabeled virus were subsequently allowed to incubate with the cells for 1 h prior to filtration. The arrow indicates the point at which the input multiplicity reached  $5 \times 10^5$  virus particles per cell.

to cell surfaces is the extent to which the reaction is specific. Generally, specific attachment is limited and therefore saturates as the amount of input material increases. In addition, attachment of labeled particles to specific sites on the cell surface can be competed by unlabeled particles, and this is shown for MVM binding in Fig. 2, curve A. In this case a fixed amount of labeled virus was added to the cells along with increasing amounts of unlabeled

particles. It can be seen that the amount of bound radioactivity begins to decline when the total input virus approaches  $5 \times 10^5$  input particles per cell. Due to the very high amounts of unlabeled virus required, we are unable to demonstrate complete competition. However, the results indicate that greater than 75% of the viral binding can be competed by unlabeled virus and is specific by this criteria.

It has been previously noted that parvovirus binding to erythrocytes (hemagglutination) and cellular debris could be minimized at high pH (9). Consequently, the dependence upon pH of MVM binding to A-9 cells was examined by using a spectrum of organic buffers to cover the pH range from 6.5 to 9.0 (Table 2). Figure 3 shows that the binding reaction has an optimum pH occurring near neutrality. These experiments were repeated using inorganic buffers (data not shown), and the pH optimum was between 7.0 and 7.2 for the binding reaction.

A second important indication of specific binding of virus to cellular receptors is the correlation of infectivity with virus binding. To further demonstrate that we are measuring a specific binding of virus to cells, we isolated a series of A-9 cell clones that were resistant to virus infection and tested them for the loss of virus binding.

**Resistance A-9 cells.** Resistance of A-9 clones to MVM infection was measured by using a modified 50% tissue culture infective dose assay for the production of viral hemagglutinin. Table 3 shows the data for comparison of infection of control A-9 cells and the clonal derivative designated 8-E. The cells were infected by ad-

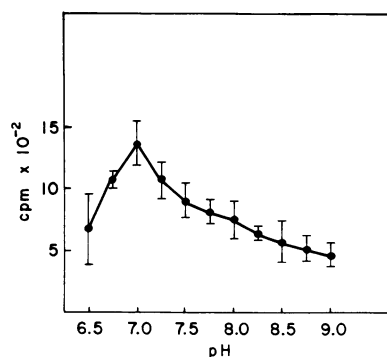


FIG. 3. pH optimum for MVM binding reaction;  $2 \times 10^5$  A-9 cells suspended in various buffer combinations (listed in Table 2) were reacted with  $10^5$  [ $^3\text{H}$ ]thymidine-labeled viral particles per cell at  $4^\circ\text{C}$  for 2 h. The suspensions were filtered as described in the text, and the cell-associated radioactivity was determined. There is pH optimum at pH 7.0. Each point is the average of three determinations plus or minus the range.

sorption of dilutions of 110S MVM stock in PBS at  $37^\circ\text{C}$  for 2 h. The control A-9 cells produce the expected dilution-dependent curve in terms of hemagglutination activity (Fig. 4). By comparison, it appears that the 8-E cells require a 5-log-unit-higher concentration of input virus than do the control A-9 cells to produce the same amount of hemagglutinin. The 50% tissue culture infective dose curve for the normal cells peaks in the middle, demonstrating the cell growth dependence of viral production. At the highest multiplicity of infection a larger percentage of cells is initially infected and consequently inhibited from further cell division. Cells infected at a lower multiplicity of infection can go through several cell growth cycles prior to spread of the infection to all of the cells. The infection was allowed to proceed for 4 days to confluency, explaining the lower titers of viral protein at the lowest multiplicities of infection.

In Fig. 5 virus-binding saturation curves generated in parallel on normal A-9 and resistant 8-E cells are shown. The A-9 curve is biphasic, consisting of a specific, saturable component saturating at approximately  $5 \times 10^5$  virus particles bound per cell and an apparently nonspecific insaturable component. Virus binding to the 8-E cells is monophasic and insaturable under this condition, mimicking the nonspecific portion of the A-9 virus-binding curve. The 8-E cells appear to have lost the specific virus receptor present in  $5 \times 10^5$  copies per A-9 cell.

Figure 6 is a saturation curve comparing the permissive A-9 cell line and the nonpermissive L1210 line. In the case of the permissive A-9

TABLE 2. Buffer solutions used to generate Fig. 3<sup>a</sup>

Buffer <sup>b</sup>	pK <sub>a</sub>	Concn used (mM)	pH used
BIS Tris	6.46	20	6.50
PIPES	6.80	10	6.75; 7.00
BES	7.15	20	7.25
TES	7.50	20	7.50
HEPES	7.55	20	7.75
HEPPS (EPPS)	8.00	20	8.00
Tricine	8.15	20	8.25
Bicine	8.35	20	8.50
Tris	8.30	20	8.75; 9.00

<sup>a</sup> Each buffer solution also contained 0.9% NaCl,  $7 \times 10^{-4}$  M  $\text{CaCl}_2$ , and  $5 \times 10^{-4}$  M  $\text{MgCl}_2$ .

<sup>b</sup> BIS, *N,N*-methylenebisacrylamide; PIPES, piperazine-*N,N'*-bis(2-ethanesulfonic acid); TES, *N*-tris(hydroxymethyl)methyl-2-aminomethane-sulfonic acid; HEPES, *N*-2-hydroxyethyl piperazine-*N'*-2-ethanesulfonic acid; BES, *N,N*-bis(2-hydroxyethyl)-2-aminoethane sulfonic acid; HEPPS, *N*-2-hydroxyethylpiperazine propane sulfonic acid.

TABLE 3. Hemagglutination activity produced in a tissue culture infectivity assay run on A-9 and 8-E cells in parallel<sup>a</sup>

Dilution of infectious stock	Hemagglutinin production			
	A-9	Mean	8-E	Mean
10 <sup>-2</sup>	64; 64; 128	85	2; 4; 4	3.3
10 <sup>-3</sup>	128; 128; 256	170	0; 0; 0	0
10 <sup>-4</sup>	128; 512; 512	384	0; 0; 0	0
10 <sup>-5</sup>	64; 64; 64	64	0; 0; 0	0
10 <sup>-6</sup>	32; 8; 8	16	0; 0; 0	0
10 <sup>-7</sup>	2; 2; 2	2	0; 0; 0	0

<sup>a</sup> A total of 10<sup>5</sup> cells were seeded into 35-mm culture dishes. Dilutions of stock MVM were adsorbed in 0.5 ml of PBS at 37°C for 2 h. The cultures were subsequently fed with growth media (see text) and refed daily. Four days after infection, mock-infected control cultures of both cell types had reached confluency. The lowest three dilution samples exhibited gross cytopathology in the A-9 cultures, whereas no growth inhibition or cytopathic effect was evident in any 8-E cultures. At this time cells were harvested into 0.01 M Tris-0.005 M EDTA (pH 9.0) buffer and lysed by sonic treatment. Viral protein was assayed by the standard hemagglutination assay.

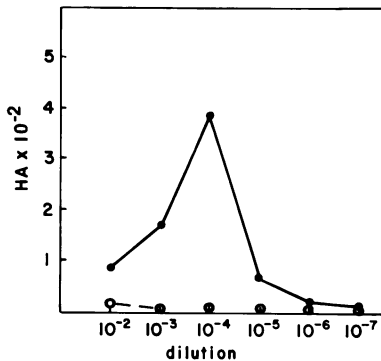


FIG. 4. Tissue culture infectivity assay performed on control A-9 cells and a resistant clone of A-9 cells designated 8-E: 10<sup>5</sup> A-9 cells or 8-E cells in monolayer were infected with the dilutions of stock virus shown by adsorption in PBS at 37°C for 2 h. After 4 days in growth media all of the 8-E cultures and several of the A-9 cultures had reached confluency. At this time, each sample was harvested into 0.01 M Tris-0.005 M EDTA (pH 9.0) buffer, sonically treated, and assayed for viral protein by the hemagglutination assay. The results are shown in Table 3, and the mean of the triplicate measurement is plotted in Fig. 5. 8-E cells produced measurable quantities of hemagglutinin only at the highest concentration of virus used, whereas A-9 cells produced hemagglutinin at all concentrations of input virus used. Symbols: A-9 (●); 8-E (○).

cells, again there is a break in the saturation curve at between  $5 \times 10^5$  and  $7 \times 10^5$  viral particles bound per cell, reflecting the number of specific binding sites. The nonpermissive L1210 line shows little appreciable binding in the concentration range used in this experiment. Much lower levels of "specific" binding may exist for the L1210 cell line, but it is in no way comparable to the A-9 system. The L1210 saturation data when plotted on a lower scale

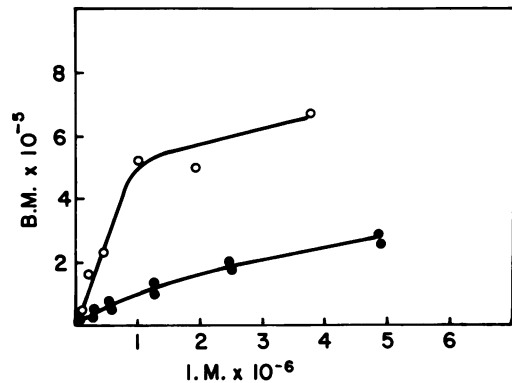


FIG. 5. Comparison of MVM binding to control A-9 cells and to resistant cloned derivatives of A-9 cells designated 8-E;  $2 \times 10^5$  A-9 or 8-E cells suspended in PBS at 4°C were reacted with the indicated multiplicity of [<sup>3</sup>H]thymidine-labeled MVM particles per cell (input multiplicity [I.M.]) for 2 h. Samples were then filtered, and the cell-associated radioactivity was measured and converted to bound multiplicity (B.M.) as described in the text. At all concentrations of input virus, filtration of cell-free control samples resulted in retention of less than 0.1% of the input radioactivity, whereas samples with cells retained up to 75%. The control A-9 cells bind virus in a biphasic manner, with saturation of the first component occurring at about  $5 \times 10^5$  MVM particles per cell and the second component not saturable under these conditions. Symbols: A-9 (○); 8-E (●).

(one log unit) generate a monophasic curve similar to the 8-E curve (not shown). This indicates that the L1210 cells also bind virus with nonsaturating kinetics. The reaction is, however, of even lower affinity than observed for virus binding by 8-E cells.

In view of the reports that specific tissues are susceptible to parvovirus infection during the course of development (3, 12), it was of interest

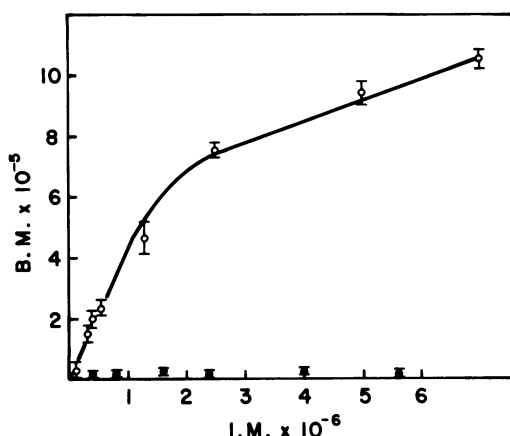


FIG. 6. Comparison of MVM binding to permissive A-9 cells and to nonpermissive L-1210 cells:  $2 \times 10^5$  cells (A-9 or L-1210) suspended in PBS at  $4^\circ\text{C}$  were reacted with the indicated number of [ $^3\text{H}$ ]thymidine-labeled MVM particles per cell (input multiplicity [I.M.]) for 2 h. Samples were then filtered, and the cell-associated radioactivity was measured and converted to bound multiplicity (B.M.) as described in the text. Symbols: A-9 (○); L-1210 (●). Each point is the average of three determinations plus or minus the range.

to determine if the number of viral attachment sites changed in cells undergoing "differentiation." Friend-745 erythroleukemia cells can be induced to differentiate and produce hemoglobin in culture with  $\text{Me}_2\text{SO}$  (6). These cells are permissive for MVM growth in uninduced cultures (16a). Friend cells appear to be a stem cell in the erythropoietic series, which ultimately leads in vivo to formation of mouse erythrocytes. These erythrocytes bind and are agglutinated by the virus. In view of these facts, we wished to determine if the number of virus-binding sites per cell changes during the induced differentiation of these cells in culture. A culture of uninduced Friend cells was split into two equal volumes of fresh media, one of which received 1.8%  $\text{Me}_2\text{SO}$ . Induction was measured by counting the percentage of benzidine (hemoglobin)-positive cells in each culture. Initially both cultures were less than 1% benzidine positive, and the uninduced culture remained as such throughout successive days. The induced culture steadily increased in the proportion of benzidine-positive cells, reaching a peak of 50% on day 4. Cells were harvested and suspended in cold PBS, and the virus-binding assay as described for A-9 cells above (see also Materials and Methods) was used to titrate the number of specific binding sites per cell in the parallel cultures. Figure 7 shows that both induced and uninduced cul-

tures possess about  $1.5 \times 10^5$  saturable binding sites per cell, and no difference between the two is detectable with our methods.

**Electron microscopy.** In an attempt to visualize the virus-binding sites on the surface of the cell, A-9 cells in monolayer were exposed to  $10^6$  virus particles per cell in PBS at  $4^\circ\text{C}$  for 2 h. The monolayers were rinsed and prepared for electron microscopy as described in Materials and Methods. Due to virus adsorption to the substrate (unpublished observations) as well as equilibrium considerations (see Fig. 5 and 6), fewer than  $5 \times 10^5$  particles are bound per cell under these conditions. MVM can be seen to bind to at least three morphologically distinct regions of the surface (Fig. 8 and 9). First of all, clusters of virus, as well as single particles, can be seen on the surfaces of numerous filopodia. Small patches of particles, as well as single particles, can also be seen scattered over the apparently unspecialized regions of the cell surface. In addition, virus particles can be seen localized in specialized clefts in the cell membrane. These clefts are characterized by a prominent submembranous thickening and outer surface glycocalyx and appear to be endocytotic regions of the cell surface (1, 7).

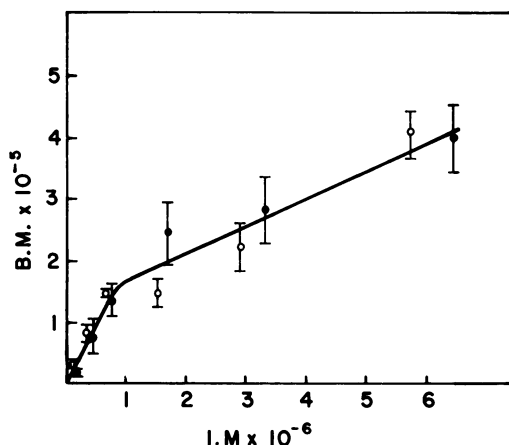
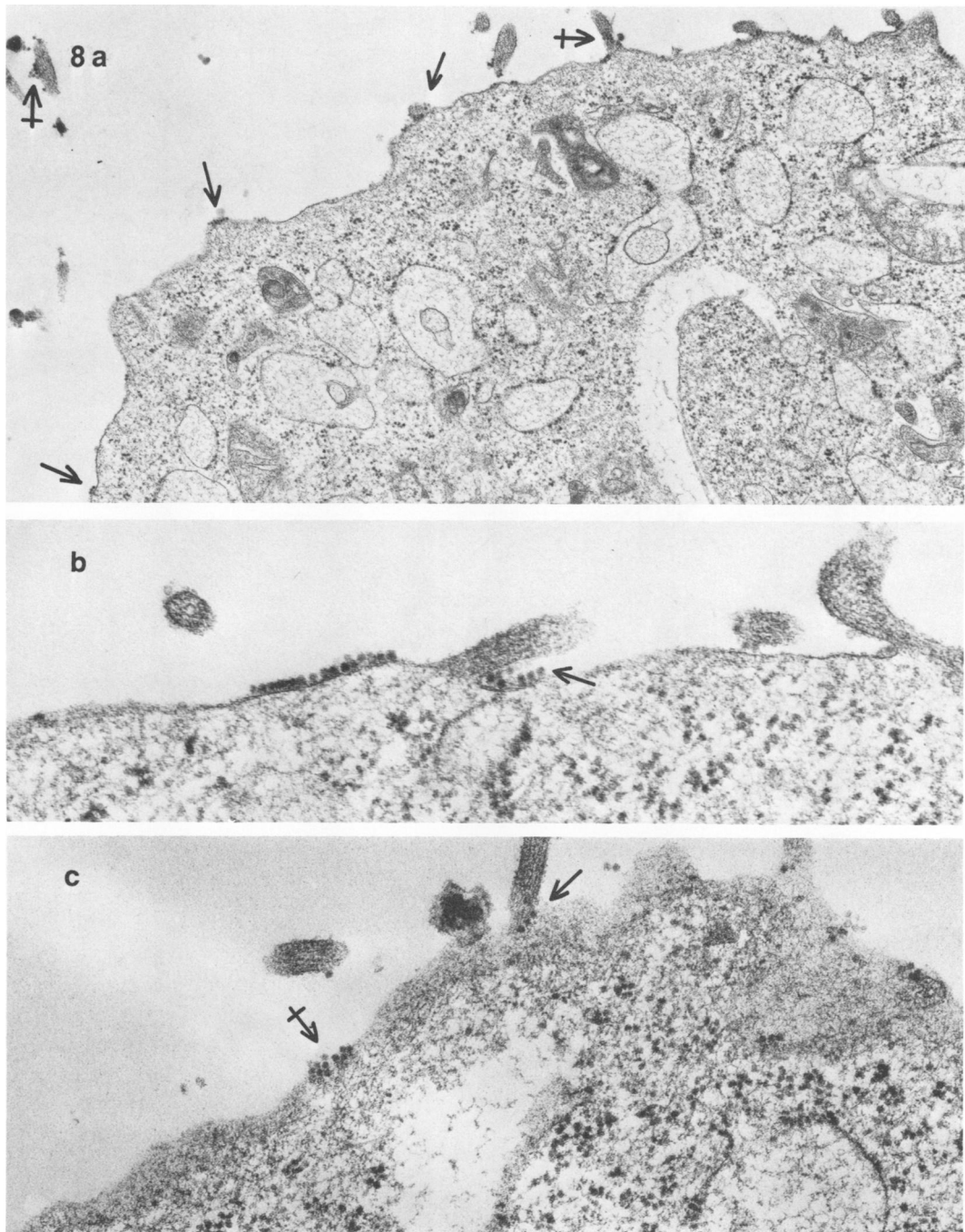


FIG. 7. Comparison of saturation binding of MVM to induced and uninduced Friend-745 erythroleukemic cells:  $2 \times 10^5$  induced or uninduced Friend-745 cells (Fig. 8) suspended in PBS at  $4^\circ\text{C}$  were reacted with the indicated number of [ $^3\text{H}$ ]thymidine-labeled particles (input multiplicity [I.M.]) for 2 h. Samples were then filtered, and the bound multiplicity (B.M.) was measured as described in the text. Both induced and uninduced cultures bind virus with a biphasic curve, which goes through a transition at approximately  $1.5 \times 10^5$  saturable binding sites per cell. Symbols: uninduced Friend-745 cells (○); induced Friend-745 cells (●). Each point is the average of three determinations plus or minus the range.



**FIG. 8.** Electron micrographs of the surface of A-9 cells fixed after a 2-h exposure to  $10^6$  110S MVM particles per cell at  $4^{\circ}\text{C}$ . (a) Low magnification of A-9 cell showing several scattered patches of adsorbed MVM. The arrows indicate a few such patches. The crossed arrows point out clusters of virions adhering to filipodia.  $\times 18,000$ . (b) High-magnification micrograph showing a large patch of MVM bound to the cell surface. The section was apparently cut perpendicular to the plane of the cell membrane at the region of the virus patch. This area of the membrane appears to be relatively unspecialized morphologically. An additional patch of virus can be seen to continue from the flat cell surface up the stalk of a filipodium (arrow)  $\times 60,000$ . (c) Electron micrograph showing virus bound to filipodia (arrow) as well as a tangential section through a virus patch illustrating the paracrystalline nature of such patches at the cell surface (crossed arrow).  $\times 45,000$ .



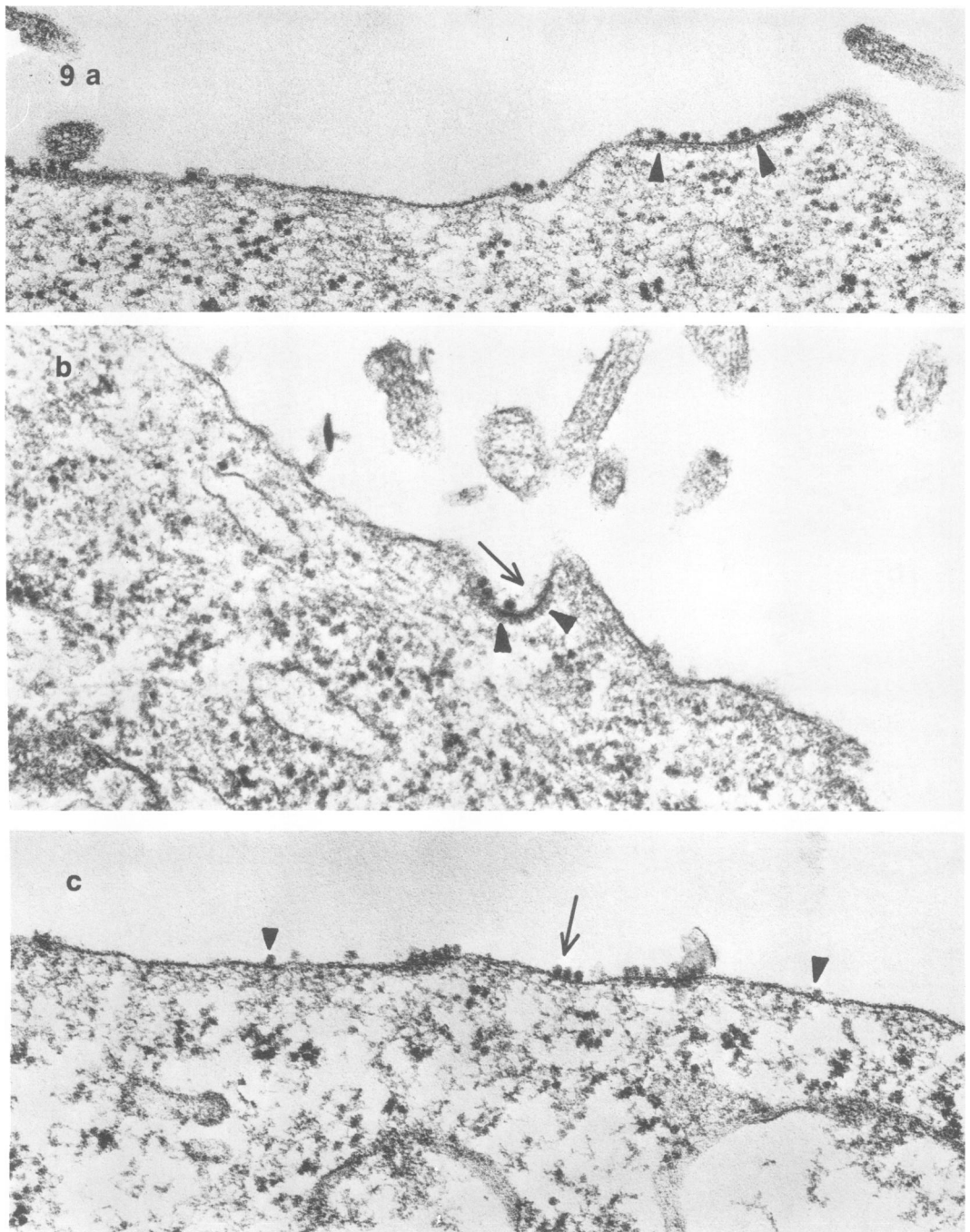


FIG. 9. Electron micrographs of the surface of A-9 cells prepared as in Fig. 8. (a) Micrograph showing virus bound to unspecialized regions of surface membrane as well as to a morphologically distinguishable region of membrane. This specialized region is characterized by a prominent thickening on the inside (arrow heads) and a less clearly visible glycocalyx on the outside surface of the plasmalemma.  $\times 60,000$ . (b) Micrograph again showing virus particles adsorbed to a specific membrane region characterized by a prominent submembranous thickening (arrow heads) and lightly visible outer glycocalyx (arrow).  $\times 65,000$ . (c) MVM particles adsorbed to unspecialized regions of cell surface in groups (arrow) and as single particles (arrow heads).  $\times 60,000$ .



These results demonstrate that when the viral receptor sites are in excess, virus is observed on several regions of the cell surface. Further studies are in progress to delineate the processes by which the bound virus enters the cell.

## DISCUSSION

Utilizing a radiolabeled virus probe, we have characterized and quantified the number of "specific" MVM binding sites on the surface of several murine cell lines. The A-9 derivative of mouse L-cells (13) binds virus with a biphasic saturation curve and a pH optimum of 7.2 at 4°C. The biphasic saturation curve can be broken into a rapidly saturable and an apparently insaturable reaction. There are approximately  $5 \times 10^5$  saturable binding sites on A-9 cells. Friend-745 erythroleukemic cells, another murine cell line permissive for MVM growth (16a), also bind virus in a biphasic reaction with approximately  $1.5 \times 10^5$  saturable binding sites per cell. The mouse lymphoid cell line L1210, however, is not susceptible to MVM infection and binds little virus. A cloned variant of the A-9 cell line selected for resistance to infection with MVM was also developed and shown to apparently lack the saturable component of the biphasic binding curve. These results indicate that the saturable and, consequently, specific binding sites on A-9 cells are directly involved in the infectious process.

Most of the cell-associated counts following a binding reaction at 4°C are at the surface of the cell and not internalized. About 80% of the cell-associated counts can be washed off the cell with a brief exposure to  $\text{Ca}^{2+}$ ,  $\text{Mg}^{2+}$ -free PBS containing 0.001 M EDTA. After a 2-h incubation with subsaturating quantities of labeled virus, at least 45% of the counts can be removed from the cell in a 1-h chase with excess cold virus. This last observation suggests that the binding of MVM at 4°C is reversible and will consequently approach equilibrium.

Rough estimates of the initial rate of attachment were calculated from the slope of the binding curves ( $K$ ) at 30 s, as described by Lonberg-Holm and Whiteley (16). At 4°C the value equals  $2.8 \times 10^{-7} \text{ cm}^3/\text{min}$ , and at 21°C  $K$  equals  $4.4 \times 10^{-7} \text{ cm}^3/\text{min}$ . This represents an increase in  $K$  by a factor of 1.33/10°C. This is very close to the predicted effects of temperature on the diffusion coefficient for particles this size (i.e., 1.30/10°C) (16, 22). Thus, the difference seen between reactions occurring at 4 and 21°C seem to be due primarily to the change in particle diffusion rates. Also, since the phase transition for membrane lipids occurs

at 18°C (K. Lonberg-Holm and L. Phillipson, in Tiffany and Blough, ed., *Cell Membranes and Viral Envelopes*, in press), it does not appear that the binding of MVM as measured here requires free lateral movement of receptors, contrary to what has been reported for adenovirus (17).

The binding of several different picornaviruses, as well as adenovirus, is affected somewhat more by temperature than MVM binding (16), although there is considerable variability (2, 11). The initial rates of attachment for MVM calculated at 4 and 21°C are considerably more rapid than for picornaviruses in general (i.e.,  $10^{-8}$  to  $10^{-9} \text{ cm}^3/\text{min}$  at 30 to 37°C) (16). The theoretical maximum rate of  $1.7 \times 10^{-7} \text{ cm}^3/\text{min}$  for picornaviruses (16) is also somewhat slower than observed for MVM. This may reflect the crudeness of our rate measurements. On the other hand, this may be due at least in part to the considerable differences that exist between the picornavirus-receptor relationship and MVM-receptor interactions. Picornaviruses bind to  $10^4$  receptors per cell, whereas MVM receptors appear to be about 50 times as numerous, which would increase the rate of parvovirus binding by increasing the number of effective cell-virus collisions. The picornavirus receptor reaction has been generally reported as being largely irreversible. MVM binding measured at 4°C is, however, readily reversible and apparently defined by second-order equilibrium kinetics.

The virus preparations used to measure the above findings were well suited for these purposes. The virus was radiolabeled with [ $^3\text{H}$ ]thymidine to avoid such changes in the surface properties of the virus as might be produced by techniques such as radiolabeling with iodine. The virus is isolated in velocity gradients to assure that the particles are monodisperse when introduced into a reaction, an important consideration in view of the tendency for MVM to aggregate when placed into a high-salt environment such as CsCl equilibrium density gradients. Once the virus has been placed into physiological salt concentrations as in the binding reaction mixtures, it is impossible to control aggregation, and this may contribute to the nonspecific component of the binding reaction.

The purity of the virus probe was confirmed by sodium dodecyl sulfate-discontinuous gel electrophoresis (18). Only viral proteins are observed in the 110S material from the sucrose velocity gradients. All of the radioactivity is acid precipitable and resistant to DNase. These observations indicate that all of the cell-associated radioactivity after a binding reac-

tion indeed represents adsorbed or internalized virus.

The results of the binding of virus to induced and uninduced Friend-745 cells indicate that the virus-binding sites do not change on the surface, although during  $\text{Me}_2\text{SO}$ -induced differentiation the cell surface undergoes several alterations with the appearance of new antigens (8). Whereas the viral attachment sites are present in the extreme form of the differentiated cell *in vivo*, the mouse erythrocyte, our results indicate that virus-binding sites are probably retained throughout the differentiation process in about the same numbers per cell as present on the precursor cells. Furthermore, in light of these results it is unlikely that the uninduced cultures of Friend-745 cells support growth of MVM due to the presence of a few spontaneously induced cells that have viral receptors among a large population of resistant cells lacking receptors.

It is worth noting that an erythroid tumor line possesses virus-binding sites whereas the lymphoid tumor line (L1210) appears to lack receptors. The difference between lymphoid and erythroid cells in terms of MVM infection susceptibility has been previously noted by Miller et al. (16a).

Preliminary electron microscopic examination of virus bound to A-9 cells in subsaturating quantities reveals binding to several morphologically distinct regions of the cell surface. A comprehensive study utilizing specific virus labeling is under way to shed further light on the nature of the specific, infection-related binding sites.

The data we have presented on the binding of MVM to cells can be explained by a simple model: cells sensitive to viral infection bind virus to specific sites on the surfaces; some virus is also bound nonspecifically, but such binding is very inefficient in causing infection of the cell. However, it should be noted that our viral probe consists of the full virus class of particles, which is not homogeneous. The 110S virus consists of at least two classes of particles: a low but variable percentage (5 to 25%) of a dense ( $1.46 \text{ g/cm}^3$  in CsCl) precursor particle and a high percentage of a lighter ( $1.42 \text{ g/cm}^3$  in CsCl) product particle (4, 18). Some evidence has been presented which might indicate that the minor, dense species has a poor affinity for cells compared with the binding of the major species (4). In our experiments, we have observed up to 60 to 65% of the input particles bound to cells when sites are in excess. These results would support the idea that our binding assay measures the binding of the predominant

$1.42\text{-g/cm}^3$  density class particles. However, recent results indicate that both classes of viral particles are equally rapidly bound to cells under our assay conditions (P. Linser and R. W. Armentrout, *in* D. C. Ward and P. Tattersall, ed., *Parvoviruses*, in press). The fact that the viral preparations used in the binding assay are not homogeneous limits the conclusions that can be derived from the kinetic data.

Nevertheless, the heterogeneity of the viral particle preparations does not affect our conclusion that specific cell surface receptors are required for efficient infection of cells.

#### ACKNOWLEDGMENTS

We gratefully acknowledge helpful discussions with Peter Tattersall and David Ward during the course of this work. R. Morris provided expert technical assistance.

This investigation was supported by Public Health Service grants 1 K04 CA 00134 and 5 R01 CA-16517 awarded by the National Cancer Institute, grant 1-396 from the National Science Foundation-March of Dimes, and a grant from the United Fund Health Foundation of Canton, Ohio.

#### LITERATURE CITED

1. Anderson, R. G. W., J. L. Goldstein, and M. S. Brown. 1976. Localization of low density lipoprotein receptors on plasma membrane of normal human fibroblasts and their absence in cells from a familial hypercholesterolemia homozygote. *Proc. Natl. Acad. Sci. U.S.A.* 73:2434-2438.
2. Bachtold, J. G., H. C. Bubel, and L. P. Gebhart. 1957. The primary interaction of Poliomyelitis virus with host cells of tissue culture origin. *Virology* 4:582-589.
3. Bates, R. C., and J. Storz. 1973. Host cell range and growth characteristics of bovine parvoviruses. *Infect. Immun.* 7:398-402.
4. Clinton, G. M., and M. Hyashi. 1976. The parvovirus MVM: a comparison of heavy and light particle infectivity and their density conversion *in vitro*. *Virology* 74:57-63.
5. DeBernardo, S., M. Weigle, V. Toome, K. Manhart, and W. Leimgruber. 1974. Studies on the reaction of fluorescamine with primary amines. *Arch. Biochem. Biophys.* 163:390-399.
6. Friend, C., W. Scher, J. G. Holland, and T. Sato. 1971. Hemoglobin synthesis in murine virus-induced leukemic cells *in vitro*: stimulation of erythroid differentiation by dimethyl sulfoxide. *Proc. Natl. Acad. Sci. U.S.A.* 68:378-382.
7. Friend, D. S., and M. G. Farquhar. 1967. Functions of coated vesicles during protein absorption in the rat vas deferens. *J. Cell Biol.* 35:357-376.
8. Fujihama, N., Y. Sujimoto, and A. Hajiwaru. 1973. Induction of erythroid maturation by DMSO in Friend leukemia cells. *Dev. Growth Differ.* 15:141.
9. Gierthy, J. F., K. A. O. Ellem, and I. I. Singer. 1974. Environmental pH and the recovery of H-1 parvovirus during single cycle infection. *Virology* 60:548-557.
10. Holland, J. J., and B. H. Hoyer. 1962. Early stages of enterovirus infection. *Cold Spring Harbor Symp. Quant. Biol.* 27:101-112.
11. Holland, J. J., and L. C. McLaren. 1959. The mammalian cell-virus relationship. II. Adsorption, reception and eclipse of parvovirus by HeLa cells. *J. Exp. Med.* 109:487-504.

12. Kilham, L., and G. Margolis. 1970. Pathogenicity of minute virus of mice for rats, mice, and hamsters. *Proc. Soc. Exp. Biol. Med.* 133:1447-1452.
13. Littlefield, J. W. 1964. Three degrees of guanylic acid-inosinic acid pyrophosphorylase deficiency in mouse fibroblasts. *Nature (London)* 203:1142-1144.
14. Lonberg-Holm, K., R. L. Crowell, and L. Phillipson. 1976. Unrelated animal viruses share receptors. *Nature (London)* 259:679-681.
15. Lonberg-Holm, K., and B. D. Korant. 1972. Early interaction of rhinoviruses with host cells. *J. Virol.* 9:29-40.
16. Lonberg-Holm, K., and N. M. Whiteley. 1976. Physical and metabolic requirements for early interactions of poliovirus and human rhinovirus with HeLa cells. *J. Virol.* 19:857-870.
- 16a. Miller, R. A., D. C. Ward, and F. H. Ruddle. 1977. Embryonal carcinoma cells (and their somatic hybrids) are resistant to infection by murine parvovirus MVM which does infect other teratocarcinoma-derived cell lines. *J. Cell. Physiol.* 91:393-401.
17. Phillipson, L., E. Everitt, and K. Lonberg-Holm. 1976. Molecular aspects of virus-receptor interaction in the adenovirus system. In R. F. Beers, Jr., and E. G. Bassett (ed.), *Cell membrane receptors for viruses, antigens and antibodies, polypeptide hormones, and small molecules*. Raven Press, New York.
18. Richards, R., P. Linser, and R. W. Armentrout. 1977. The kinetics of assembly of a parvovirus, minute virus of mice, in synchronized rat brain cells. *J. Virol.* 22:778-793.
19. Rose, J. A. 1974. Parvovirus reproduction, p. 1-61. In H. Fraenkel-Conrat and R. R. Wagner (ed.), *Comprehensive virology*, vol. 3. Plenum Press, New York.
20. Tattersall, P. 1972. Replication of the parvovirus MVM. I. Dependence of virus multiplication and plaque formation on cell growth. *J. Virol.* 10:586-590.
21. Tattersall, P., P. J. Cawte, A. J. Shatkin, and D. C. Ward. 1976. Three structural polypeptides coded for by minute virus of mice, a parvovirus. *J. Virol.* 20:273-289.
22. Valentine, R. C., and A. C. Allison. 1959. Virus particle adsorption. I. Theory of adsorption and experiments on the attachment of particles to non-biological surfaces. *Biochim. Biophys. Acta* 34:10-23.